# Inversion of Electromagnetic Induction Log in Anisotropic Media using an Adjoint Integral Equation Method

Saputera, D.H.; Jakobsen, M.; Jahani, N.; van Dongen, K.W.A.; Alyaev, S.; Eikrem, K.S.

**DOI**
10.3997/2214-4609.2024101259

**Publication date**
2024

**Document Version**
Final published version

**Citation (APA)**
Saputera, D. H., Jakobsen, M., Jahani, N., van Dongen, K. W. A., Alyaev, S., & Eikrem, K. S. (2024). *Inversion of Electromagnetic Induction Log in Anisotropic Media using an Adjoint Integral Equation Method*. Paper presented at 85th EAGE Annual Conference & Exhibition 2024, Oslo, Lillestrøm, Norway. https://doi.org/10.3997/2214-4609.2024101259

# Inversion of Electromagnetic Induction Log in Anisotropic Media using an Adjoint Integral Equation Method

D.H. Saputera[1], M. Jakobsen[1], N. Jahani[2], K.W.A. Van Dongen[3], S. Alyaev[2], K.S. Eikrem[2]

[1] University Of Bergen; [2] NORCE Norwegian Research Centre; [3] Delft University of Technology

## Summary

Inversion of electromagnetic induction log while drilling provides structural information around borehole for geosteering decision process. Imaging a complex three-dimensional (3D) anisotropic formation is very challenging due to the significant cost of the forward solver. To overcome this challenge, we have developed an inversion algorithm using an adjoint Integral Equation Method for logging while drilling scenarios in anisotropic media with several inexpensive approaches in this study. We use a quasi-Newton method with L-BFGS algorithm and implement a matrix-free adjoint Integral Equation method for efficient update of inverted model parameters. In addition, we propose the use of limited number of iterations for solving the adjoint equation as an approximation to the gradient for a faster computation time. To regularize the inverted models, we adopt the use of multiplicative regularization and weighted L2 total variation. Additionally, we impose priori information in our formulations, such as 2D parameterization and the range of conductivity values. We show a numerical example of logging while drilling inversion on a 2.5D faulted anisotropic formation. Numerical experiments show that our inversion workflow shows a good structural agreement of the inverted model within the sensitive range of the tool.

# Inversion of Electromagnetic Induction Log in Anisotropic Media using an Adjoint Integral Equation Method

## Introduction

Electromagnetic (EM) induction logging tools are commonly used to assist the optimal trajectory decision process while drilling. The tool typically has multiple axial components with different sensitivities to the subsurface structure and anisotropy. Three-dimensional (3D) inversion of induction logs enables imaging of complex geological formations (Puzyrev et al., 2019). However, it is still very challenging because of the significant computational cost of the 3D forward modelling. This motivates the study of inexpensive approaches to the inverse problem.

In this study, we have developed an inversion algorithm using an adjoint Integral Equation Method for logging while drilling scenarios in anisotropic media with several inexpensive approaches. The inversion is done by minimizing an objective function using a quasi-Newton method with the L-BFGS algorithm (Liu and Nocedal, 1989). This method only requires the objective function gradient to update the parameters. For efficient gradient calculations, we adopted the matrix-free variant of the Distorted Born Iterative (DBI) and adjoint method (Jakobsen et al., 2023). In addition, we tested the using a limited number of GMRES (Saad, 2003) iterations for solving the adjoint equation as an approximation to the gradient for a faster computation time. We adopt the use of multiplicative regularization and weighted L2 total variation (Van Den Berg and Abubakar, 2001) which enables adaptive regularization parameters and edge preservation of the inverted model. Additionally, we impose priori information in our formulations, such as 2D parameterization and the range of conductivity values.

We focus on the implementation of a tilted vertical transverse isotropic (VTI) medium where the drilling trajectory is at a certain angle to the anisotropic structure. We show a numerical example of logging while drilling inversion on a 2.5D faulted anisotropic formation. To demonstrate inversion while drilling, we assume a moving simulation and inversion window with the drilling tools. The conductivity inverted from the previous window is used as the initial model in the overlapping zone between two windows. Numerical experiments show that our inversion workflow shows a good structural agreement of the inverted model within the sensitive range of the tool. Since we use a 3D forward solver, our implementation can be straightforwardly generalized into the 3D problem.

## Theory

**Forward Model**. We use the Integral Equation (IE) method to compute the magnetic fields at receiver locations. In the IE method, we solve the following equations (Zhdanov, 2009):

$$\mathbf{E}^{(b)}(\mathbf{r}) = \mathbf{E}^{(0)}(\mathbf{r}) + \int_{\Omega} \mathbf{G}^{(0,E)}(\mathbf{r},\mathbf{x}')\,\Delta\boldsymbol{\sigma}(\mathbf{x}')\mathbf{E}^{(b)}(\mathbf{x}')\ d^3\mathbf{x}', \tag{1}$$

$$\mathbf{H}^{(b)}(\mathbf{r}) = \mathbf{H}^{(0)}(\mathbf{r}) + \int_{\Omega} \mathbf{G}^{(0,H)}(\mathbf{r},\mathbf{x}')\,\Delta\boldsymbol{\sigma}(\mathbf{x}')\mathbf{E}^{(b)}(\mathbf{x}')\ d^3\mathbf{x}', \tag{2}$$

where $\mathbf{E}$, $\mathbf{H}$ denote the electric and magnetic fields, $\mathbf{G}$ indicates the Green's function, and $\mathbf{r}$ is the receiver locations. The upper scripts (0) and (b) refer to the fields and Green's function defined for homogeneous isotropic medium and heterogeneous anisotropic medium, respectively. $\Omega$ is the domain with the conductivity contrast $\Delta\boldsymbol{\sigma}(\mathbf{x}) = \boldsymbol{\sigma} - \sigma_0\mathbf{I}$ with $\boldsymbol{\sigma}$ the actual anisotropic medium and the $\sigma_0$ background medium and $\mathbf{I}$ the identity tensor. The electric Green's tensor $\mathbf{G}^{(0,E)}$ and the magnetic Green's tensor $\mathbf{G}^{(0,H)}$ are (Fang et al., 2006)

$$\mathbf{G}^{(0,E)} = \left(i\omega\mu_0\,\mathbf{I} + \frac{\nabla\nabla}{\sigma_0}\right) g(\mathbf{x},\mathbf{x}'), \text{ and } \mathbf{G}^{(0,H)} = (i\omega\mu_0)^{-1}\nabla\times\mathbf{G}^{(0,E)}, \tag{3}$$

where $g(\mathbf{x},\mathbf{x}') = \frac{e^{ik_0|\mathbf{x}-\mathbf{x}'|}}{4\pi|\mathbf{x}-\mathbf{x}'|}$ is the scalar Green's function with $k_0^2 = i\omega\mu_0\sigma_0$, $i = \sqrt{-1}$, $\omega$ is the angular frequency, and $\mu_0$ is the magnetic permeability of free space. The subsurface model is discretized into a set of grid blocks and the electric fields in the heterogenous medium are obtained by solving the following linear system of equations

$$\left(\mathbf{I} - \mathbf{G}^{(0,E)}\Delta\boldsymbol{\sigma}\right)\mathbf{E}^{(b)} = \mathbf{E}^{(0)}, \tag{4}$$

which can be solved efficiently using Krylov subspace-based iterative solvers and the FFT convolution algorithm. Afterward, the magnetic fields at the receiver positions can be calculated directly from equation (2). For more details on our implementation, we refer to the paper of Saputera et al. (2023).

**Model Parameterization.** The conductivity tensor $\boldsymbol{\sigma}$ of a tilted VTI medium to the drilling angle in the 2.5D inversion frame can be expressed as(Gao, 2006)

$$\boldsymbol{\sigma} = \mathbf{R}^{\mathrm{T}} \begin{bmatrix} \sigma_1 & 0 & 0 \\ 0 & \sigma_1 & 0 \\ 0 & 0 & \sigma_2 \end{bmatrix} \mathbf{R}, \text{ and } \mathbf{R} = \begin{bmatrix} \cos\alpha & 0 & -\sin\alpha \\ 0 & 1 & 0 \\ \sin\alpha & 0 & \cos\alpha \end{bmatrix}, \tag{5}$$

where $\mathbf{R}$ is a rotation tensor, $\sigma_1$ and $\sigma_2$ correspond to the horizontal and vertical conductivity in the global coordinate frame, respectively, with $\alpha$ the drilling angle. To impose conductivity boundaries, we propose the following model parameterization (Abubakar et al., 2006):

$$\sigma_{\mathrm{k}} = 0.5(\sigma_{\max} + \sigma_{\min}) + 0.5(\sigma_{\max} - \sigma_{\min}) \sin(\mathrm{m}_{\mathrm{k}}), \ \mathrm{k} = 1{,}2, \tag{6}$$

where $m$ is the inverted model parameters. For 2.5D inversion, we set the model such that it is invariant in the y-direction. To include this condition, we can parameterize the model with $\boldsymbol{m}_{3\mathrm{D}} = \mathbf{P}\boldsymbol{m}_{2\mathrm{D}}$ where $m_{2\mathrm{D}}$and $m_{3\mathrm{D}}$ indicate a vector that describes the model parameters distribution in the 2D and 3D space, respectively, and $\mathbf{P}$ is an operator that maps the conductivity from 2D to 3D space. In this study, we simply use an $N_{3D} \times N_{2D}$ matrix of ones for this purpose.

**Inversion Objective Function**. We adopt the use of the multiplicative objective function described in Van Den Berg and Abubakar (2001)

$$\Phi = \Phi_{\mathrm{D}} \cdot \Phi_{\mathrm{TV}}, \tag{7}$$

where $\Phi_{\mathrm{D}}$ is the weighted data misfit and $\Phi_{\mathrm{TV}}$ is the total variation regularization cost. The advantage is that the data misfit adaptively determines the regularization weighting parameter. To minimize this objective function, we use a built-in MATLAB function with a quasi-Newton algorithm and L-BFGS algorithm as the inverse Hessian approximation (Liu and Nocedal, 1989).

**Weighted Data Misfit**. The weighted data misfit is defined as the weighted difference between the observed and calculated magnetic fields ($\mathbf{H}^{(\mathrm{b,obs})}$ and $\mathbf{H}^{(\mathrm{b,calc})}$, respectively):

$$\Phi_{\mathrm{D}} = 0.5 \cdot \langle \mathbf{W}\Delta\mathbf{H}, \mathbf{W}\Delta\mathbf{H} \rangle_{\mathrm{D}}, \tag{8}$$

$$\Delta\mathbf{H} = \mathbf{H}^{(\mathrm{b,obs})} - \mathbf{H}^{(\mathrm{b,calc})}, \tag{9}$$

with $\langle\cdot,\cdot\rangle_{\mathrm{D}}$ denotes the scalar product in the data space and $\mathbf{W}$ is the weight that is defined as the inverse Frobenius norm of the magnetic fields at receiver positions with different configurations:

$$\mathbf{W}(\mathbf{r}_{\mathrm{j}}) = \left\|\mathbf{H}^{(\mathrm{obs})}\right\|_{\mathrm{F}}^{-1}, \ \mathrm{j} = 1{,}2, \ldots, \ \mathrm{N}_{\mathrm{receiver}}, \tag{10}$$

where $\mathbf{r}$ is the receiver position and F is the Frobenius norm. The derivative of $\Phi_{\mathrm{D}}$ with respect to the isotropic conductivity using the adjoint rule can be written as:

$$\frac{\partial \Phi_D}{\partial \sigma}(\mathbf{x}) = \mathrm{Re}\left\langle -\mathbf{E}^{(\mathrm{b})}(\mathbf{x}), \left[\mathbf{G}^{(\mathrm{b,H})}\right]^{\dagger} \mathbf{W}^2 \Delta\mathbf{H} \right\rangle_{\mathrm{D}}, \tag{11}$$

where $\mathbf{G}^{(\mathrm{b,H})}$ denotes the 'heterogeneous background' Magnetic fields Green's function is defined as

$$\mathbf{G}^{(\mathrm{b,H})} = \mathbf{G}^{(0,\mathrm{H})}\left[\mathbf{I} + \Delta\boldsymbol{\sigma}\left(\mathbf{I} - \mathbf{G}^{(0,\mathrm{E})}\Delta\boldsymbol{\sigma}\right)^{-1}\mathbf{G}^{(0,\mathrm{E})}\right]. \tag{12}$$

We define the adjoint electric field as $\mathbf{E}^{(\mathrm{a})} = \left[\mathbf{G}^{(\mathrm{b,H})}\right]^{\dagger}\mathbf{W}^2\Delta\mathbf{H}$ which is backpropagated from the source receivers to the inversion domain. The gradient of the weighted data misfit function is the correlation between the total and adjoint electric fields. Calculating equation (11) involves solving the adjoint problem of equation (4). This costs additional forward solver calls when using an iterative solver. Hence, we propose to use a few iterations when solving the adjoint problem. Using the scattering potential decomposition technique (Jakobsen et al., 2023) on the conductivity tensor and chain rule, the derivative with respect to the 2.5D model parameterization is written as

$$\frac{\partial \Phi_{\mathrm{D}}}{\partial \mathrm{m}_k}(\mathbf{x}_{\mathbf{m}}) = \frac{\partial \sigma_{\mathrm{k}}}{\partial \mathrm{m}_k}(\mathbf{x}_{\mathbf{m}}) \odot \mathbf{P}^{\mathrm{T}}\mathrm{Re}\left\langle -\mathbf{E}^{(\mathrm{b})}(\mathbf{x}), \mathbf{R}^{\mathrm{T}}\mathbf{B}_{\mathrm{k}}\mathbf{R}\mathbf{E}^{(\mathrm{a})}(\mathbf{x})\right\rangle_{\mathrm{D}}, \ \mathrm{k} = 1{,}2, \tag{13}$$

$$\mathbf{B}_1 = \begin{bmatrix} 1 & 0 & 0 \\ 0 & 1 & 0 \\ 0 & 0 & 0 \end{bmatrix} \text{ and } \mathbf{B}_2 = \begin{bmatrix} 0 & 0 & 0 \\ 0 & 0 & 0 \\ 0 & 0 & 1 \end{bmatrix}, \tag{14}$$

where $\mathbf{x_m}$ denotes the space of the model parameters and $\odot$ is the elementwise multiplication. $\mathbf{P}^{\mathrm{T}}$ is the transpose of the mapping operator and its action is summing over the y-direction in our study case.

**Weighted L2 Regularization.** We chose to regularize the log of conductivity to equalize the difference in the resistive and conductive regions. Following Van Den Berg and Abubakar (2001), we write the weighted L2 total variation as:

$$\Phi_{\mathrm{TV}}^{(\mathrm{n})}[\sigma_{\mathrm{k}}] = \frac{1}{\mathrm{V}} \int_{\Omega} \frac{\left|\mathrm{W}_{\mathrm{TV}}^{(\mathrm{n}-1)}(\mathbf{x}) \boldsymbol{\nabla} \log[\sigma_{\mathrm{k}}(\mathbf{x})]\right|^2 + \delta^{(\mathrm{n}-1)}}{\left|\mathrm{W}_{\mathrm{TV}}^{(\mathrm{n}-1)}(\mathbf{x}) \boldsymbol{\nabla} \log[\sigma_{\mathrm{k}}(\mathbf{x})^{(\mathrm{n}-1)}]\right|^2 + \delta^{(\mathrm{n}-1)}} \mathrm{d}^3\mathbf{x}, \ \mathrm{k}= 1,2, \tag{15}$$

where V is the volume or area that encloses the inversion domain $\Omega$, $n$ is the iteration number. $\delta$ is a perturbation factor defined as $\delta^{(\mathrm{n}-1)} = \gamma \Phi_{\mathrm{D}}^{(\mathrm{n}-1)} (\Delta)^{-2}$ with $\Delta$ the grid size and $\gamma$ a relaxation parameter controls how much the inverted model is regularised. If there is no update, then $\gamma$ is increased by a factor of two. $\mathrm{W}_{\mathrm{TV}}$ is a weighting term to avoid regularization beyond the tool's sensitivity. This weight depends on the gradient of the data misfit specified in the following:

$$\mathrm{W}_{\mathrm{TV}}^{(\mathrm{n}-1)}(\mathbf{x}) = \max\left[\left|\frac{\partial \Phi_{\mathrm{D}}}{\partial \sigma_1}^{(\mathrm{n}-1)}\right|(\mathbf{x}), \left|\frac{\partial \Phi_{\mathrm{D}}}{\partial \sigma_2}^{(\mathrm{n}-1)}\right|(\mathbf{x})\right] \cdot \left(\max\left[\left|\frac{\partial \Phi_{\mathrm{D}}}{\partial \sigma_1}^{(\mathrm{n}-1)}\right|, \left|\frac{\partial \Phi_{\mathrm{D}}}{\partial \sigma_2}^{(\mathrm{n}-1)}\right|\right]\right)^{-1}. \tag{16}$$

The total variation regularization cost is then the sum of the weighted L2-norm of both parameters:

$$\Phi_{\mathrm{TV}} = \Phi_{\mathrm{TV}}[\sigma_1] + \Phi_{\mathrm{TV}}[\sigma_2]. \tag{17}$$

## Numerical Examples and Discussion

Figure 1. shows a schematic of the moving simulation and inversion window. This window is moving along with the induction tool and the grid points inside the windows coincide with each other. Each simulation window is discretized into 32 x 32 x 32 grid blocks with a size of 1 x 1 x 1 $\mathrm{m}^3$. We simulate induction logs across faulted anisotropic formations with an $80^{\mathrm{o}}$ drilling angle as shown in Figure 2a and 2c. The transmitter spacing is 2 m and there are 126 logging positions in total. The transmitter has frequencies of 12, 24, and 48 kHz with three receivers 5, 10, and 15 m behind the transmitter. We set homogeneous isotropic background conductivity $\sigma_0 = 0.1$ S/m for all simulations and add 2% uniformly distributed random noise to the data.

The inversion is done sequentially using the data at one logging position at a time. The inverted model in all positions initialized equal to the conductivity of the previous window in the overlapping region and equal to $\sigma_0$ in the other region. We set the inverted conductivity boundaries between 0.1 $\sigma_0$ – 10 $\sigma_0$. When solving the adjoint problem, we use ten GMRES (Saad, 2003) iterations for faster calculation time. Additionally, we implement the frequency hopping strategy where the data is inverted from the low- to high-frequency data (Van Den Berg and Abubakar, 2001). The inversion is stopped when the norm of the data misfit normalized with the norm of the observed data is less than 0.02. This process can be repeated back-forth from the starting to the end position so that the data misfit calculated from the latest inversion results gives a better match in all positions. Figure 2 shows the model obtained from eleven forward and backward repetitions of the sequential inversion. The process took approximately 10 hours on a laptop with AMD Ryzen 7 4800H CPU and NVIDIA GeForce RTX 3060 Laptop GPU.

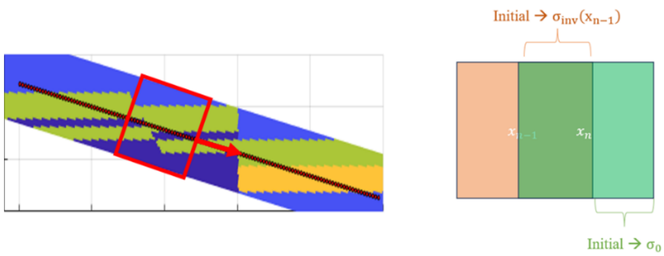


***Figure 1** Sketch of the moving forward modelling and inversion window.*

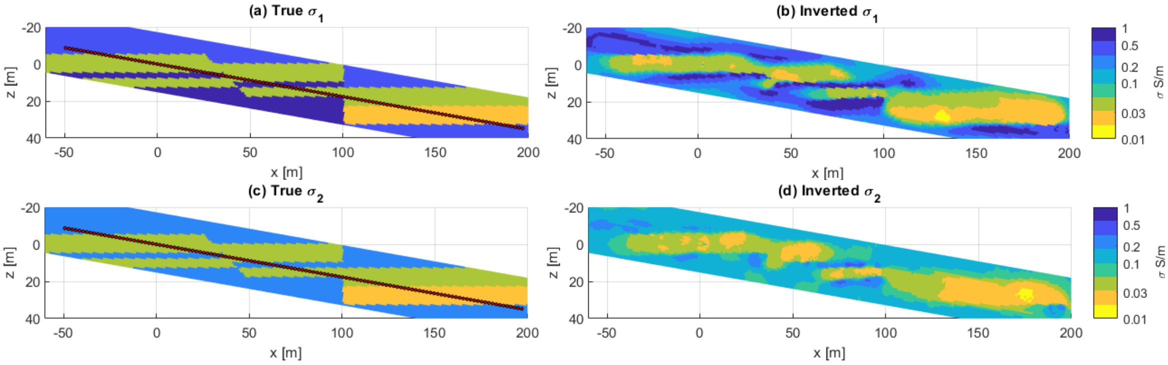

*__Figure 2__ The x-z plane view of the true and inverted model parameters. $\sigma_1$ and $\sigma_2$ refer to the horizontal and vertical conductivity, respectively. The dots are the transmitter positions.*

The inverted model shows a similar structure close to the drilling trajectory. Qualitatively, the model is better reconstructed in the resistive area compared to the conductive area and the $\sigma_1$ is better recovered compared to the $\sigma_2$. This may be related to the limited sensitivity of the tool configurations.

**Conclusions**

We have developed an efficient inversion algorithm using an adjoint Integral Equation Method for logging while drilling scenarios in anisotropic media. We use several inexpensive approaches including the quasi-Newton method with L-BFGS algorithm and limited GMRES iteration for solving the adjoint problems. In the future study, we aim to optimize the inversion workflow by including different assimilation strategies between the inversion window and a priori knowledge about the anisotropic media for better convergence and inversion results, especially for dealing with 3D structures.

**Acknowledgements**

This work is part of the Center for Research-based Innovation DigiWells: Digital Well Center for Value Creation, Competitiveness and Minimum Environmental Footprint (NFR SFI project no. 309589, https://DigiWells.no). It is funded by the Research Council of Norway, Aker BP, Equinor, Lundin Energy, ConocoPhillips, TotalEnergies, Vår Energi, and Wintershall Dea.

**References**

Abubakar, A., Habashy, T. M., Druskin, V., Knizhnerman, L., and Davydycheva, S. [2006]. A 3D parametric inversion algorithm for triaxial induction data. Geophysics, 71(1), G1–G9.
Fang, S., Gao, G., and Verdin, C. T. [2006]. Efficient 3D Electromagnetic Modelling in the Presence of Anisotropic Conductive Media, Using Integral Equations. Exploration Geophysics, 37(3), 239–244.
Gao, G. [2006]. Simulation of borehole electromagnetic measurements in dipping and anisotropic rock formations and inversion of array induction data. The University of Texas at Austin.
Jakobsen, M., Xiang, K., and Van Dongen, K. W. A. [2023]. Seismic and medical ultrasound imaging of velocity and density variations by nonlinear vectorial inverse scattering. The Journal of the Acoustical Society of America, 153(5), 3151.
Liu, D. C., and Nocedal, J. [1989]. On the limited memory BFGS method for large scale optimization. Mathematical Programming, 45(1–3), 503–528.
Puzyrev, V., Pardo, D., Calo, V., and Torres-Verdín, C. [2019]. Recent advances on the inversion of deep directional borehole resistivity measurements. ASEG Extended Abstracts, 2019(1), 1–3.
Saad, Y. [2003]. Iterative methods for sparse linear systems. SIAM.
Saputera, D. H., Jakobsen, M., van Dongen, K. W. A., Jahani, N., Eikrem, K. S., and Alyaev, S. [2023]. 3-D induction log modelling with integral equation method and domain decomposition pre-conditioning. Geophysical Journal International, 236(2), 834–848.
Van Den Berg, P. M., and Abubakar, A. [2001]. Contrast Source Inversion Method: State of Art. Progress In Electromagnetics Research, 34, 189–218.
Zhdanov, M. S. [2009]. Geophysical electromagnetic theory and methods. Elsevier.